transient cooling the local temperatures near a boundary are lower than in the interior. The temperature variation is more pronounced for large κ_D and when n is near 1; this makes ε_{fd} much different from ε_{ut}. As n increases, internal reflections make the temperature distribution more uniform and ε_{fd} approaches ε_{ut}. For a fixed n, ε_{ut} increases with κ_D; for ε_{fd} however, there is a maximum for $\kappa_D \approx 2$.

The characteristics of the fully developed temperature distribution are in Fig. 2. The normalized shape of $F(X)$ is in Fig. 2a; it is rather insensitive to both n and κ_D. The effect of n on the shape is increased for larger κ_D values. The amplitude $F(1/2) - F(0) = F(1/2) - 1$ is in Fig. 2b. It increases substantially with κ_D if n is near 1. When $n = 4$, the amplitude is considerably reduced.

Conclusions

Fully developed transient emittances were obtained for a radiating layer cooling by exposure to a cold vacuum environment. The layer has diffuse surfaces and a refractive index $n \geq 1$. Emittances were evaluated from a similarity solution that was found to exist during transient cooling. As the layer temperature distribution decreases with time, its normalized shape becomes fixed for each set of parameters. The normalized shape is a weak function of n and κ_D. The fully developed transient emittances have a considerably different behavior than those for a uniform temperature layer. From the transient solutions in Ref. 1, the ε_{fd} provides a lower emittance limit during transient cooling for the present conditions.

References

[1]Siegel, R., "Refractive Index Effects on Transient Cooling of a Semitransparent Radiating Layer," *Journal of Thermophysics and Heat Transfer*, Vol. 9, No. 1, 1995, pp. 55–62.

[2]Siegel, R., "Separation of Variables Solution for Non-Linear Radiative Cooling," *International Journal of Heat and Mass Transfer*, Vol. 30, No. 5, 1987, pp. 959–965.

[3]Siegel, R., "Some Aspects of Transient Cooling of a Radiating Rectangular Medium," *International Journal of Heat and Mass Transfer*, Vol. 32, No. 10, 1989, pp. 1955–1966.

[4]Spuckler, C. M., and Siegel, R., "Refractive Index Effects on Radiative Behavior of a Heated Absorbing-Emitting Layer," *Journal of Thermophysics and Heat Transfer*, Vol. 6, No. 4, 1992, pp. 596–604.

Spectrally Correlated Monte Carlo Formulations for Radiative Transfer in Multidimensional Systems

J. Liu* and S. N. Tiwari†
Old Dominion University, Norfolk, Virginia 23529

Introduction

FOR the investigation of radiative heat transfer in multidimensional gaseous systems, recent efforts are being directed to employ realistic narrow-band models to represent the absorption-emission characteristics of participating species. Use of a narrow band results in several types of spectral correlations in the radiative formulations. Three different methods[1–3] have been developed to deal with these spectral correlations. Among these methods, the Monte Carlo method (MCM) has been found to have definite advantages over other methods. In Ref. 3, radiative heat transfer between two infinite parallel plates was simulated in an exact manner, and one-dimensional correlated and noncorrelated Monte Carlo formulations were developed with almost no assumptions. However, the application of this exact treatment to multidimensional problems will be extremely complicated, and numerical solutions of these formulations will be very difficult. By introducing an appropriate assumption, the complicated Monte Carlo formulations can be simplified significantly. Therefore, the objective of this study is to develop and validate the approximate correlated and noncorrelated Monte Carlo formulations that are suitable for multidimensional problems. In this study, attention is directed to a simple two-dimensional problem. The exact Monte Carlo formulations are developed first and these are utilized to obtain the approximate formulations. Following this, a comparative study is conducted to determine the net radiative wall flux and radiative source distributions by employing the exact and approximate, correlated and noncorrelated, Monte Carlo formulations.

Analysis of Monte Carlo Simulation using a Narrow-Band Model

Consider an absorbing and emitting molecular gas between two parallel plates of finite length L and height H as shown in Fig. 1a. The inlet and outlet of the gas are at the section $x = 0$ and $x = L$, respectively, and they are treated as pseudoblack walls with prescribed temperatures. Temperature, concentration, and pressure in the medium are supposed to be known. The walls are assumed to be diffuse, but not necessarily gray. The temperature distribution of each wall is also known. The radiative transfer quantities of interest in this study are the net radiative wall flux and the radiative source term inside the medium. In order to calculate these quantities,

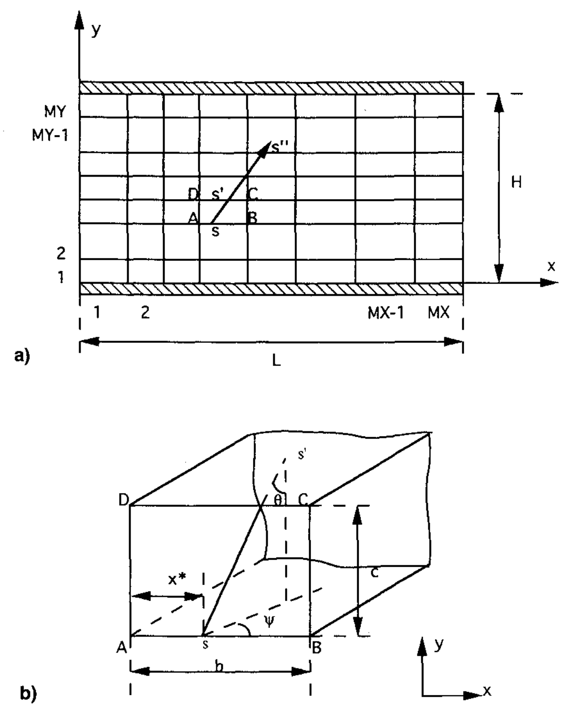

Fig. 1 Schematic of two finite parallel plates: a) coordinates system and b) volume element *ABCD*.

Received Sept. 13, 1993; revision received March 30, 1994; accepted for publication Sept. 26, 1994.

*Graduate Research Assistant, Department of Mechanical Engineering. Student Member AIAA.

†Eminent Professor, Department of Mechanical Engineering. Associate Fellow AIAA.

the medium considered is divided into an $MX \times MY$ array of rectangular volume elements (Fig. 1a). Similarly, the two real walls are each divided into MX surface elements, and the inlet and outlet pesudowalls are each divided into MY surface elements.

As in Ref. 3, the statistical narrow-band model with an exponential-tailed-inverse intensity distribution is employed in this study. Use of a narrow-band model in the MCM presents new features in the analysis of radiative heat transfer. The statistical relationships developed by Siegel and Howell[4] need to be modified to incorporate the narrow-band model. The Monte Carlo analyses presented here are based on an arbitrarily chosen finite volume element $ABCD$ (Fig. 1b), with the length and height equal to b and c, respectively. Exact correlated and noncorrelated formulations are derived first; then approximate correlated and noncorrelated formulations are developed.

Exact Correlated and Noncorrelated Monte Carlo Formulations

In this case, an energy bundle is simulated in an exact manner in terms of the narrow-band model without any approximation. Let us consider the Planck spectral blackbody intensity $I_{b\omega}$ that enters the element $ABCD$ at the point s on the side of AB and intersects one of the other three sides of the element at the point s' as shown in Fig. 1b. It should be understood that each side of the element is a surface. A spherical coordinate system is established and centered at the point s. The distance between the points s and A is x^*. From Ref. 5, the amount of energy emitted for a wave number range $d\omega$ and a pencil of column $s \to s'$ with a solid angle increment $d\Omega$ and an area increment dx^* is

$$dQ = I_{b\omega}[1 - \tau_\omega(s \to s')]\cos\theta \, d\Omega \, dx^* \, d\omega \tag{1}$$

where $\tau_\omega(s \to s')$ is the spectral transmittance over the path $s \to s'$, θ is the polar angle between the y axis and the direction of the column $s \to s'$, and $d\Omega = \sin\theta \, d\theta \, d\psi$, where ψ is the azimuthal angle. The total emitted energy calculated in terms of the intensity entering from the sides of AB $(0 < \theta \le \pi)$ and DC $(\pi < \theta \le 2\pi)$ is obtained by integrating Eq. (1) over the wave number, polar angle, azimuthal angle and area as

$$Q = \sum_{k=1}^{m_\omega} \left\{ \int_0^b \int_0^\pi \int_0^{2\pi} \overline{I_{b\omega^k}}[1 - \overline{\tau_{\omega^k}}(s \to s')]\cos\theta \sin\theta \, d\psi \, d\theta \, dx^* \right\} \Delta\omega^k \tag{2}$$

Here the narrow-band approximation has been employed to replace the real spectral transmittance with the averaged spectral transmittance over a narrow band.[2,3] The width of narrow band is $\Delta\omega$; each band is centered at ω^k and characterized by the superscript k, and m_ω is the total number of narrow bands.

In the MCM, the radiant energy is regarded as being carried by discrete energy bundles. The simulation of an energy bundle includes the determination of wave number, and starting point and direction of emission of this energy bundle in the finite volume element. The statistical relationships for determining these parameters are readily obtained from Eq. (2) as[4,5]

$$R_\omega = \left(\sum_{k=1}^{n} \left\{ \int_0^b \int_0^\pi \int_0^{2\pi} \overline{I_{b\omega^k}}[1 - \overline{\tau_{\omega^k}}(s \to s')]\cos\theta \sin\theta \, d\psi \, d\theta \, dx^* \right\} \Delta\omega^k \right) \Big/ Q$$
$$(\omega^{n-1} < \omega \le \omega^n) \tag{3}$$

$$R_{x^*} = \left(\sum_{k=1}^{m_\omega} \left\{ \int_0^{x^*} \int_0^\pi \int_0^{2\pi} \overline{I_{b\omega^k}}[1 - \overline{\tau_{\omega^k}}(s \to s')]\cos\theta \sin\theta \, d\psi \, d\theta \, dx^* \right\} \Delta\omega^k \right) \Big/ Q \tag{4}$$

$$R_\theta = \left(\sum_{k=1}^{m_\omega} \left\{ \int_0^\theta \int_0^b \int_0^{2\pi} \overline{I_{b\omega^k}}[1 - \overline{\tau_{\omega^k}}(s \to s')]\cos\theta \sin\theta \, d\psi \, dx^* \, d\theta \right\} \Delta\omega^k \right) \Big/ Q \tag{5}$$

$$R_\psi = \left(\sum_{k=1}^{m_\omega} \left\{ \int_0^\psi \int_0^b \int_0^{\pi} \overline{I_{b\omega^k}}[1 - \overline{\tau_{\omega^k}}(s \to s')]\cos\theta \sin\theta \, d\theta \, dx^* \, d\psi \right\} \Delta\omega^k \right) \Big/ Q \tag{6}$$

where R_ω, R_{x^*}, R_θ, R_ψ are random numbers that are uniformly distributed between zero and one.

To determine the absorption location of an energy bundle, consider the emitted radiant energy along a pencil of column $s \to s'$ (Fig. 1a). After this amount of energy is transmitted over a column $s' \to s''$, the remaining radiant energy is given by

$$dQ' = I_{b\omega}[1 - \tau_\omega(s \to s')]\tau_\omega(s' \to s'')\cos\theta \, d\Omega \, dx^* \, d\omega \tag{7}$$

where $\tau_\omega(s' \to s'')$ is the spectral transmittance over the path $s' \to s''$. Taking a narrow-band average of Eqs. (1) and (7), and dividing the latter by the first, the statistical relationship for determining the location of absorption can be expressed as

$$R_l = \frac{\overline{[1 - \tau_\omega(s \to s')]\tau_\omega(s' \to s'')}}{1 - \overline{\tau_\omega}(s \to s')} = \frac{\overline{\tau_\omega}(s' \to s'') - \overline{\tau_\omega}(s \to s'')}{1 - \overline{\tau_\omega}(s \to s')} \tag{8}$$

where R_l is a random number. In Eq. (8), the spectral correlation between $\tau_\omega(s \to s')$ and $\tau_\omega(s' \to s'')$ has been taken into account due to a high resolution structure in a very small range of an absorption band. Otherwise, spectrally noncorrelated formulation for R_l is obtained as

$$R_l = \overline{\tau_\omega}(s' \to s'') \tag{9}$$

Therefore, it is seen that exact correlated and noncorrelated Monte Carlo formulations differ only in the relation for R_l as given in Eqs. (8) and (9).

Approximate Correlated and Noncorrelated Monte Carlo Formulations

In the exact analysis, numerical evaluations of Eqs. (2–6) for Q, R_ω, R_{x^*}, R_θ, R_ψ involve four-dimensional integrations, and the integrands in these equations are very complex functions of integration variables. Obviously, the Monte Carlo simulation has already become very difficult, although the problem considered is a simple two-dimensional problem. To simplify complicated Monte Carlo formulations, it is assumed that the volume dV of a volume element is very small so that the energy emitted within dV escapes before reabsorption. With consideration of a narrow-band model, the total emitted radiative energy and the statistical relationships for determining the wave number and emission direction of an energy bundle are derived easily as[4,5]

$$Q_{dV} = 4\pi \sum_{k=1}^{m_\omega} (\overline{\kappa_{\omega^k}}\overline{I_{b\omega^k}}\Delta\omega^k)\, dV \tag{10}$$

$$R_\omega = \left[4\pi \sum_{k=1}^{n} (\overline{\kappa_{\omega^k}}\overline{I_{b\omega^k}}\Delta\omega^k)\, dV\right] \Big/ Q_{dV}, \quad (\omega^{n-1} < \omega \le \omega^n) \tag{11}$$

$$R_\theta = (1 - \cos\theta)/2, \qquad R_\psi = \psi/2\pi \tag{12}$$

Here, the mean absorption coefficient over a narrow band $\overline{\kappa_{\omega^k}} \approx -\ln \overline{\tau_{\omega^k}}(L_m)/L_m$, where L_m is the mean beam length of the volume element. The emission point of an energy bundle from a volume element is assumed to be the center point of the element. This assumption is justifiable in an infinitesimal volume element. It is evident that Eqs. (10–12) are much simpler than the corresponding equations for the exact treatment of the Monte Carlo simulation. These simple formulations do not change with the complexity of the problem.

To calculate R_l with consideration of the spectral correlation, the mean transmittance is replaced with the mean absorption coefficients in the denominator of Eq. (8), and by employing the infinitesimal volume approximation, there is obtained[5]

$$R_l \approx \frac{L_m}{\ln \overline{\tau_\omega}(L_m)} \left[\frac{\partial \overline{\tau_\omega}(s \to s'')}{\partial_s}\right] \tag{13}$$

Equation (13) is the approximate correlated statistical relationship for determining the location of absorption and it is different from the corresponding exact correlated formulation as given in Eq. (8). The approximate noncorrelated statistical relationship for determining the location of absorption cannot be simplified further, and it is the same as given by Eq. (9). Therefore, similar to the exact correlated and noncorrelated formulations, the approximate correlated and noncorrelated formulations differ only in the expression for R_l.

Results and Discussion

In order to validate the approximate Monte Carlo analyses and to investigate the effects of spectral correlation, a problem has been selected by referring to the work of Zhang et al.[1] The results for the net radiative wall flux and radiative source term have been obtained for four different formulations that correspond to the exact correlated, approximate correlated, exact noncorrelated and approximate noncorrelated solutions, respectively. In the problem considered, the length and height of two parallel plates are $L = 1.2$ m and $H = 0.6$ m. The two real wall emissivities are chosen to be the same and equal to 0.8. The total pressure of the gas is taken to be 1 atm. The problem considered is a nonisothermal and inhomogeneous H_2O-O_2-N_2 mixture in which the molar fraction distributions are given by

$$x_{H_2O} = 0.3\{1 - 2[(x/L) - 0.5]^2\}\{2 - [(|2y - H|)/H]\}$$
$$x_{O_2} = 0.1\{1 - 3[(x/L) - 0.5]^2\}\{2.5 - [(|2y - H|)/H]\} \tag{14}$$
$$x_{N_2} = 1 - x_{H_2O} - x_{O_2}$$

and gas temperature distribution is assumed to be

$$T(x, y) = 1000 + 1200\{1 - [(|2y - H|)/H]\}x/L \tag{15}$$

The two real walls and the inlet pseudowall are kept at a temperature of 1000 K. The outlet of the gas is open to a 300 K atmosphere, so the temperature of the outlet pseudowall is 300 K. In this problem, only H_2O is the radiatively participating species. There are five important absorption bands of H_2O. All these bands have been taken into account in this study and they consist of $m_\omega = 295$ narrow bands in the range from 150 to 7500 cm^{-1}.

In the Monte Carlo simulation, the medium is divided into 20×20 uniform finite volume elements. The computations were performed on a Sun Sparc workstation. The number of total energy bundles was chosen to be 2,000,000. The CPU times for the exact correlated, approximate correlated, exact noncorrelated and approximate noncorrelated solutions were 269, 167, 378, and 225 minutes, respectively. Obviously, the CPU times for the approximate solutions are lower than those for the exact solutions.

Figure 2 shows radiative source distribution at the middle location ($x/L = 0.5$) of the plates. It is evident that the approximate and exact correlated solutions agree very well, and so do the approximate and exact noncorrelated solutions. The approximate correlated solution appears to be slightly higher in the wall region than the exact correlated solution. The two noncorrelated solutions are far below the two correlated solutions. The results of correlated solutions demonstrate that the gas goes from a net absorber near the walls to a net emitter away from the walls. But, the noncorrelated solutions predict the gas as a net emitter in nearly all regions. The radiative source distributions at several other locations of the plates are presented in Ref. 5 and they show the same trend as exhibited in Fig. 2.

The distribution of radiative wall flux along the plates is illustrated in Fig. 3. It is seen that the wall heat flux increases at first, reaches a peak value at a location closer to the outlet, and then decreases. Such a behavior is due to the fact that, for the problem considered, the outlet region is equivalent to a cold source. This cold source has a strong effect on the radiative heat transfer in the nearby region. Among the four different solutions, the approximate correlated solution is slightly lower than the exact correlated solution, and the approximate noncorrelated solution is slightly higher than the exact noncorrelated solution. A comparison of different solutions reveals that the noncorrelated formulations predict much higher radiative energy absorbed on the walls than the correlated formulations. The difference in results may reach as high as one order of magnitude in some locations.

From the results presented, it is evident that approximate formulations can provide results comparable to the corresponding exact formulations. The noncorrelated formulations, however, predict much lower radiative source distri-

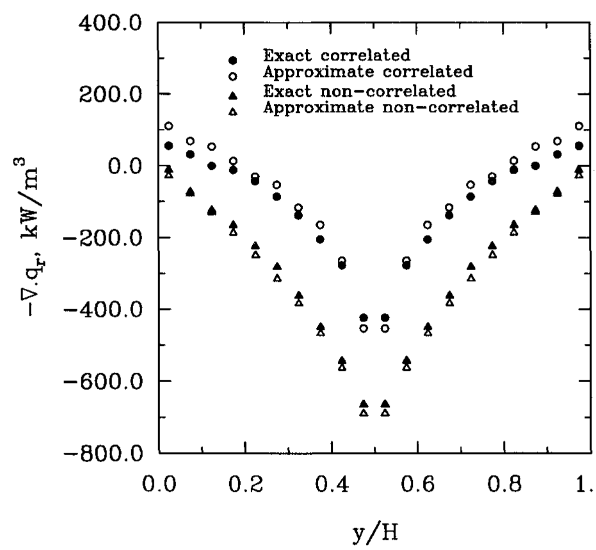

Fig. 2 Radiative source distributions at the location $x/L = 0.5$ for nonisothermal and inhomogeneous H_2O-O_2-N_2 mixture.

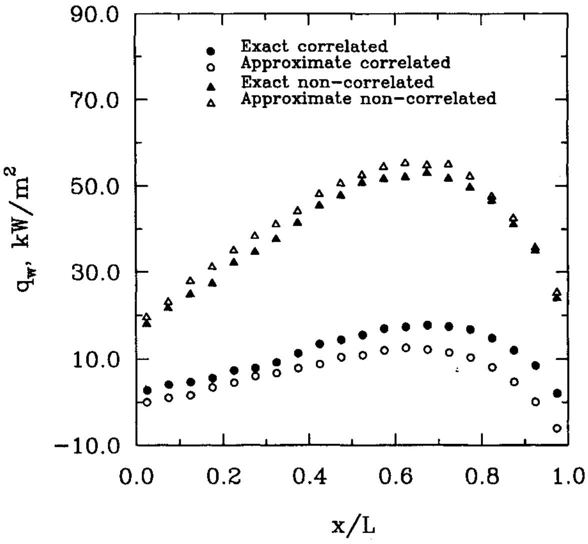

Fig. 3 Radiative wall flux distributions for nonisothermal and inhomogeneous H_2O-O_2-N_2 mixture.

bution in the medium and much higher radiative wall flux along the plates than the correlated formulations. This difference comes from the statistical relationship for determining the absorption location. The R_l calculated from the noncorrelated formulation, Eq. (9), is greater than that from the correlated formulations, Eqs. (8) and (13). Therefore, for the noncorrelated formulation, an energy bundle travels a long distance and is likely to be absorbed on the wall. This also explains why the CPU time required for the noncorrelated solution is larger than that required for the corresponding correlated solution.

Conclusions

The exact correlated and noncorrelated Monte Carlo formulations are very complicated for multidimensional systems. Solutions of these formulations are extremely difficult, if not impossible. However, by introducing the assumption of infinitesimal volume element, the approximate correlated and noncorrelated formulations are obtained, which are much simpler than the exact formulations. Consideration of different problems and comparison of different solutions reveals that the approximate and exact correlated solutions agree very well, and so do the approximate and exact noncorrelated solutions. But the two noncorrelated solutions have no physical meanings because they usually differ from the correlated solutions significantly. An accurate prediction of radiative heat transfer in any nongray and multidimensional system is possible by using the approximate correlated formulations developed in this study.

References

[1]Zhang, L., Soufiani, A., and Taine, J., "Spectral Correlated and Non-Correlated Radiative Transfer in a Finite Axisymmetric System Containing an Absorbing and Emitting Real Gas-Particle Mixture," *International Journal of Heat and Mass Transfer*, Vol. 31, No. 11, 1988, pp. 2261–2272.

[2]Menart, J. A., Lee, H. S., and Kim, T. K., "Discrete Ordinates Solutions of Nongray Radiative Transfer with Diffusely Reflecting Walls," *Journal of Heat Transfer*, Vol. 115, No. 1, 1993, pp. 184–193.

[3]Liu, J., and Tiwari, S. N., "Investigation of Radiative Transfer in Nongray Gases Using a Narrow Band Model and Monte Carlo Simulation," *Journal of Heat Transfer*, Vol. 116, No. 1, 1994, pp. 160–166.

[4]Siegel, R., and Howell, J. R., *Thermal Radiation Heat Transfer*, Hemisphere, New York, 3rd ed., 1992.

[5]Liu, J., "Radiative Interactions in Multi-Dimensional Chemically Reacting Compressible Flows," Ph.D. Dissertation, Old Dominion Univ., Norfolk, VA, 1994.

Spray Cooling Characteristics Under Reduced Gravity

Masaya Kato*
Keio University, Hiyoshi, Yokohama 223, Japan
Yoshiyuki Abe†
Electrotechnical Laboratory, Tsukuba, Ibaraki 305, Japan
and
Yasuhiko H. Mori‡ and Akira Nagashima‡
Keio University, Hiyoshi, Yokohama 223, Japan

Introduction

LIQUID spray cooling has been widely applied to many industrial processes requiring rapid and effective cooling. In space, spray cooling is expected to exhibit its outstanding potential in various thermal management systems[1] such as flash evaporators for use during re-entry, emergency cooling systems, quenching and cooling control systems for microgravity materials processing, etc. Spray cooling is, in general, thought to be rather insensitive to the variation in gravity. Nevertheless, there is experimental evidence that the heat transfer from a spray-cooled heater surface is dependent on its orientation, particularly in the transition region between the critical heat flux (CHF) point and the minimum heat flux (MHF) point, as well as in the higher surface-temperature region beyond the MHF point, and that the CHF is also under the influence of the surface orientation.[2] This fact suggests that gravity still plays some role in spray cooling.

The present study is the first attempt at evaluating the liquid spray cooling characteristics under reduced gravity conditions available in parabolic flights of an aircraft. The aircraft employed was an MU-300, a 15-m-long jet plane, which provided a reduced gravity condition of the order of 10^{-2} of the terrestrial gravity for approximately 20 s during each parabolic flight.

Experimental

The apparatus in the present experiments is schematically illustrated in Fig. 1. A liquid stored in a pressure vessel was displaced by pressurized dry nitrogen gas to generate liquid spray from the nozzle into the spray chamber, but no gas was introduced into the spray nozzle. The spray nozzle employed was a full-cone-type automobile fuel atomizer. The spray volume flux was adjusted by controlling the frequency of opening/shutting of the electromagnetic valve integrated into the nozzle, causing little change in droplet velocity. The droplet velocity was adjusted by controlling the liquid pressure in the pressure vessel. The liquid sprayed was either CFC-113 or water.

Figure 2 depicts the structure of the copper block used as the heated target to be spray-cooled. The copper block was heated up to a prescribed temperature (up to 320°C) by seven 750-W cartridge heaters embedded in the block, and then cooled down transiently by the liquid sprayed onto its nickel-plated surface, 19 mm in diameter, facing the nozzle. Ten parabolic flights were provided in a day, and the experiments started at the highest temperature and cooled down in the course of 10 parabolas. The total time for this operation was about 60 min.

Received June 24, 1994; revision received Aug. 25, 1994; accepted for publication Oct. 21, 1994.

*Graduate Student, Department of Mechanical Engineering.
†Senior Researcher, Energy Materials Section.
‡Professor, Department of Mechanical Engineering.